Preparation of Hexagonal-Close-Packed Colloidal Crystals of Hydrophilic Monodisperse Gold Nanoparticles in Bulk Aqueous Solution

ARTICLE *in* CHEMISTRY OF MATERIALS · MAY 2003

Impact Factor: 8.35 · DOI: 10.1021/cm0217147

3 AUTHORS, INCLUDING:

Keisaku Kimura
Hosei University
186 PUBLICATIONS **3,691** CITATIONS

Preparation of Hexagonal-Close-Packed Colloidal Crystals of Hydrophilic Monodisperse Gold Nanoparticles in Bulk Aqueous Solution

Suhua Wang, Seiichi Sato, and Keisaku Kimura[1]

Department of Material Science, Graduate School of Science, Himeji Institute of Technology, 3-2-1 Koto, Kamigori-cho, Ako-gun, Hyogo 678-1297, Japan

Received November 13, 2002. Revised Manuscript Received March 11, 2003

In this paper, we report on the successful preparation and characterization of large Au colloidal crystals using hydrophilic Au nanoparticles as the building units in bulk aqueous solution. Scanning electron microscopy observation shows that the Au colloidal crystals have a clear crystal appearance and well-developed facets. Elemental composition of the Au colloidal crystals is estimated using energy-dispersive X-ray spectroscopy. The crystallographic data are uniquely determined using small-angle X-ray diffraction and transmission electron diffraction. On the basis of the crystallographic data, the stacking behavior of the Au nanoparticles in the colloidal crystals is also discussed. In the three-dimensional superlattices, Au nanoparticles are hexagonal close-packed and interconnected maybe by interparticle chemical bonding thanks to the mercaptosuccinic acid molecules over the Au nanoparticle surface.

Introduction

Recently, much effort has been directed at preparing two- or three-dimensional ordered arrays, namely, colloidal crystals, nanoparticle crystals, or nanocrystal superlattices, using inorganic nanoparticles as a building block by self-assembly.[1−20] An important feature of the well-defined ordered solid is the double periodicity: the atomic periodicity in the Angstrom range and the superlattice periodicity on the nanometer scale. The properties of such double periodical superstructures can be tailored in a subtle way compared to those of simple crystals or single particles by controlling the nanoparticle core size, the chemical nature of coating organic ligands, and the arrangement of nanoparticles in the arrays. The colloidal crystal provides opportunities to investigate the collective properties different from individual nanoparticles and the coupling/interaction between nanoparticles interconnected by the coating organic molecules. Therefore, the self-assembly of nanoparticles into ordered arrays provides a route to new nanostructured materials with optimized and enhanced properties and future optical and electronic devices. Because gold nanoparticles have potential applications in electronics and biology, some effort has been directed at construction of three-dimensional structures using gold particles.[14,16,18,19] In this paper, we report the large faceted Au colloidal crystals which have been produced by homogeneous nucleation in bulk aqueous solution. The morphologies and crystallographic data of the three-dimensional nanoparticle superlattices are determined using scanning electron microscopy (SEM), high-resolution transmission electron microscopy (HRTEM), transmission electron diffraction (TED), and small-angle X-ray diffraction (XRD).

Experimental Section

Materials. The following reagents were all used as received: from Wako Pure Chemical Co., hydrogen tetrachloroaurate tetrahydrate ($HAuCl_4 \cdot 4H_2O$, 99%), mercaptosuccinic acid ($HOOCCH_2CH(SH)COOH$, 97%), methanol (99.8%), ethanol (99.5%), and other organic solvents, which are all of reagent grade; from Merck Chemical Co., sodium borohydride (NaBH4, >96%).

* Corresponding author. E-mail: kimura@sci.himeji-tech.ac.jp.

(1) Murray, C. B.; Kagan, C. R.; Bawendi, M. G. *Science* **1995**, *270*, 1335.
(2) Harfenist, S. A.; Wang, Z. L. Alvarez, M. M.; Vezmar, I.; Whetten, R. L. *J. Phys. Chem.* **1996**, *100*, 13904.
(3) Fink, J.; Kiely, C. J.; Bethell, D.; Schiffrin, D. J. *Chem. Mater.* **1998**, *10*, 922.
(4) Lin, X. M.; Sorensen, C. M.; Klabunde, K. J. *Chem. Mater.* **1999**, *11*, 198.
(5) Martin, J. E.; Wilcoxon, J. P.; Odinek, J.; Provencio, P. *J. Phys. Chem. B* **2000**, *104*, 9475.
(6) Harfenist, S. A.; Wang, Z. L.; Whetten, R. L.; Vezmar, I.; Alvarez, M. M. *Adv. Mater.* **1997**, *9*, 817.
(7) Wang, Z. L. *Adv. Mater.* **1998**, *10*, 13.
(8) Kang, H.; Jun, Y. W.; Park, J. R.; Lee, K. B.; Cheon, J. *Chem. Mater.* **2000**, *12*, 3530.
(9) Motte, L.; Billoudet, F.; Lacaze, E.; Douin, J.; Pileni, M. P. *J. Phys. Chem. B* **1997**, *101*, 138.
(10) Collier, C. P.; Vossmeyer, T.; Heath, J. R. *Annu. Rev. Phys. Chem.* **1998**, *49*, 371.
(11) Taleb, A.; Russier, V.; Courty, A.; Pileni, M. P. *Phys. Rev. B* **1999**, *59*, 13350.
(12) Sun, S.; Murray, C. B. *J. Appl. Phys.* **1999**, 85, 4325.
(13) Murray, C. B.; Kagan, C. R.; Bawendi, M. G. *Annu. Rev. Mater. Sci.* **2000**, *30*, 545.
(14) Kimura, K.; Sato, S.; Yao, H. *Chem. Lett.* **2001**, 372.
(15) Shevchenko, E. V.; Talapin, D. V.; Rogach, A. L.; Kornowski, A.; Haase, M.; Weller, H. *J. Am. Chem. Soc.* **2002**, *124*, 11480.
(16) (a) Sato, S.; Yamamoto, N.; Yao, H.; Kimura, K. *Mater. Res. Soc. Symp. Proc.* **2002**, *703*, 375. (b) Sato, S.; Yao, H.; Kimura, K. *Physica E*, in press.
(17) Lieber, M. *Nano Lett.* **2002**, *2*, 81.
(18) Stoeva, S. I.; Klabunde, K. J.; Sorensen, C. M.; Dragieva, I. *J. Am. Chem. Soc.* **2002**, *124*, 2305.
(19) Prasad, B. L. V.; Stoeva, S. I.; Sorensen, C. M.; Klabunde, K. J. *Langmuir* **2002**, *18*, 7515.
(20) Puntes, V. F.; Zanchet, D.; Erdonmez, C. K.; Alivisatos, A. P. *J. Am. Chem. Soc.* **2002**, *124*, 12874.

10.1021/cm0217147 CCC: $25.00
Published on Web 00/00/0000 PAGE EST: 3.7

Preparation of Hydrophilic Au Nanoparticles. The water-soluble mercaptosuccinic acid (MSA)-coated Au nanoparticles used as the building units of the Au colloidal crystals were prepared using a procedure basically similar to that described in previous work[21] but largely modified for mass production. Under vigorous stirring and ultrasonic irradiation 80 mL of freshly prepared 0.3 M $NaBH_4$ aqueous solution was added to a water−methanol mixture containing 1.00 g of $HAuCl_4 \cdot 4H_2O$ and 0.73 g of MSA. After the reduction reaction, a flocculent precipitate was collected by decanting the supernatant solution and then washed three times with a water−methanol mixture (volume ratio of 1:3) by repeating the resuspension and recentrifugation process. The process is repeated an additional three times with 99.8% methanol to remove unbound MSA or Au−MSA complexes. The resulting brown mushy precipitate was dispersed in 15 mL of distilled water and then was dialyzed against the flow of freshly distilled water for about 8 h. The suspension was dried by lyophilization and followed by evacuating on a vacuum line ($<5 \times 10^{-3}$ Torr) for 24 h. About 0.6 g of black powder was finally obtained. The mean diameter of the Au nanoparticles was determined to be 3.7 nm with a fwhm of 0.5 nm using TEM (Figure 1A).

Fabrication of Au Colloidal Crystals. The as-prepared Au nanoparticle powder was dispersed in distilled water to form brown solutions with a mass concentration of ≈2.0 mg/mL. The pH value of the suspension was adjusted to be 0.6 using 6.0 M HCl aqueous solution. Then the solution samples were filtered through a syringe-driven microfilter with 0.22-μm pore size immediately before they were stored in sealed glass vials to prevent the evaporation of solvent. The glass vials were kept from apparent shaking and direct irradiation of any light. After 4 days under room temperature, crystallization took place, giving numerous faceted crystals with micrometer sizes. These gold colloidal crystals were transferred carefully to Si(100) substrates for XRD and SEM experiments and to a copper support grid of amorphous carbon film for TEM and TED experiments. All of the samples were dried under vacuum to remove the remaining solvents before characterization and analysis.

Instrumentation. X-ray diffraction experiments were carried out on a Rigaku Rint 2000 diffractometer with Cu Kα radiation (λ = 1.5418 Å) operated at 40 kV and 20 mA. Scanning electron microscopy experiments and energy-dispersive X-ray analysis were performed on a Philips XL 20 scanning electron microscope. Transmission electron microscopy images were obtained using a Hitachi-8100 transmission electron microscope, under the operating voltage of 200 kV. The transmission electron diffraction patterns were recorded with a camera length of 2.0 m.

Results and Discussion

Figure 1B shows the SEM images of faceted colloidal crystals made from Au nanoparticles 3.7 nm in diameter. Clearly, the superlattices exhibit distinct shape, sharp faceted features of quality crystals. The lack of vagueness and noncharging SEM images of the colloidal crystals imply that the Au colloidal crystals may be electrical conducting. The cross dimensions of the Au colloidal crystals are measured to be ≈6−16 μm and the thickness is estimated to be ≈2−5 μm based on the SEM image depth. The majority are plate crystals with apparent triangular or hexagonal morphologies. Some other Au colloidal crystals, however, have the diamond-like shapes as indicated by "a" in Figure 1B. It should be noted that the large two crystal plates marked "b" are broken into small fragments during the handling process. The various shapes are developed when the growth rates in different directions of the crystals are different. The growth rate in the direction normal to the top surface of the plate crystals is slower than those in other directions. The direction normal to the top surface of the plate crystals is the [0001] zone axis of the hcp system as demonstrated in the following discussion.

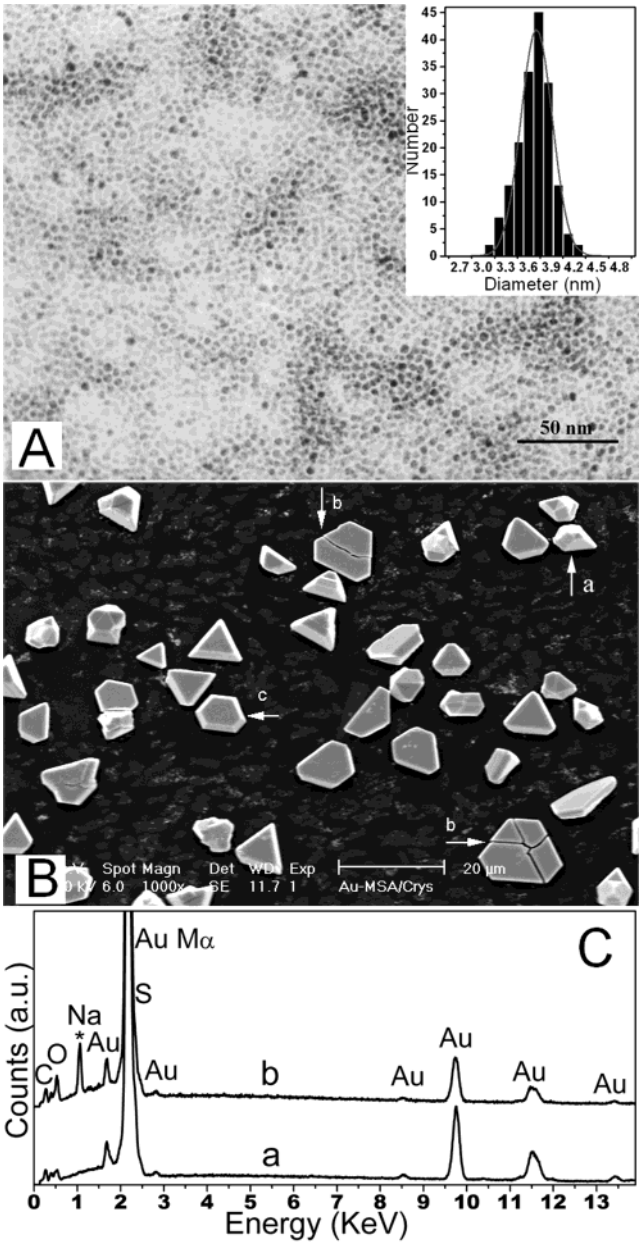

Figure 1. (A) TEM image of the MSA-coated gold nanoparticles for crystallization. The inset presents the particle size histogram of sample number 173. (B) SEM image of the faceted Au colloidal crystals on Si(100) substrate prepared in bulk aqueous solution. Arrow "a" indicates a diamond-like crystal and "b" the plate crystals broken into fragments. (C) EDX spectra recorded from Au nanoparticle powder (trace b) and the Au colloidal crystal labeled "c" in (B) (trace a).

The elemental composition of these faceted crystals is qualitatively determined using energy-dispersive X-ray (EDX) spectroscopy by performing the measurement on each individual crystal possessing triangular, hexagonal, or diamond-like shape. The results show that all crystals have elemental composition similar to that of the predominant Au component accompanied by some carbon and oxygen contents (Figure 1C, trace a). The sulfur component from the MSA molecules is not clearly

(21) Chen, S.; Kimura, K. *Langmuir* **1999**, *15*, 1075.

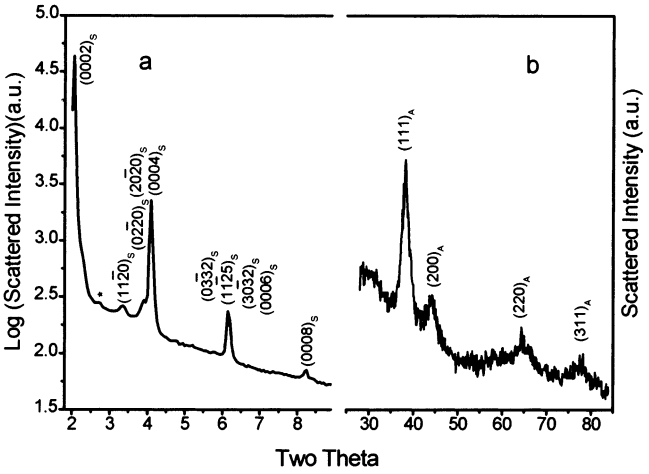

Figure 2. Powder XRD patterns recorded at a small-angle range (a) and a wide-angle range (b) with an expanded scale in ordinate from the same Au colloidal crystal sample. The subscript S of the Miller-Bravais indices means from the superlattice and subscript A of the Miller indices means from the atomic lattice of Au nanoparticles.

observed because of its peak position (2.31 keV) being overlapped with the strong peak of Au Mα (2.13 keV). For comparison, EDX experiment is also performed on Au nanoparticle powder before the crystallization (Figure 1C, trace b). Clearly, trace b is similar to trace a except for one more peak of sodium and the sodium component can be attributed to the sodium salt of MSA in the Au nanoparticle powder. Because the final pH value of the media is larger than 8.0 during the Au nanoparticle preparation, the MSA molecules coating Au nanoparticle cores are in the form of sodium salt. The crystallization, however, is carried out in a solution with ≈0.3 M HCl. In such strong acidic conditions, MSA molecules transform into acid states from sodium salts, resulting in the disappearance of sodium in the colloidal crystals. This finding suggests a hydrogen-bonding network among the MSA molecules. Trace b also suggests relatively higher carbon and oxygen contents in Au nanoparticle powder than in colloidal crystal, indicating there is some free MSA sodium salt residue in the nanoparticle powder before crystallization.

To determine the crystallographic data of the Au colloidal crystals, small-angle electron diffraction and X-ray diffraction experiments were carried out. XRD can address the structural information for a large portion of the sample, while the transmission electron diffraction can provide structural information for selected areas of the sample. Trace b in Figure 2 shows the powder X-ray diffraction pattern in a wide-angle range recorded from the colloidal crystals. X-ray diffraction peaks from atomic Au lattices of the nanoparticles are clearly seen, although there is much background noise. Trace a in Figure 2 is recorded from the same colloidal crystal sample at small angles, and the XRD pattern in the small-angle region is directly related to the ordered assembly of the nanoparticles. The small-angle XRD pattern indicates a hexagonal-close- or face-centered-cubic packing of the Au nanoparticles. The position marked with an asterisk cannot be associated with any diffraction from either the hcp system or the cubic-close-packing systems. This contribution may be attributed to a small amount of stacking faults in some colloidal crystals.

The main XRD pattern is successfully indexed as hexagonal close packing of gold nanoparticle with the parameter of $a = 5.25$ nm. However, the same XRD peaks can also be successfully indexed as face-centered-cubic (fcc) packing with $a = 7.46$ nm. Because the recorded small-angle XRD pattern does not provide enough structural information due to possible preferred orientation of the colloidal crystals and weak diffraction peak intensity, the above XRD experiment does not uniquely determine the colloidal crystals with either hexagonal close packing or cubic close packing. Therefore, a selected area small-angle TED technique was adapted to collect further crystallographic data for structural determination.

To obtain a statistical result, the selected area TED experiments were performed on randomly sampled individual colloidal crystals having triangular, hexagonal, or diamond-like shapes. The TED experiment is unsuccessful on the crystals with diamond-like shape owing to their large thickness. But very clear TED patterns can be obtained from triangular-shaped or hexagonal-shaped plate crystals. The TED patterns recorded from 12 randomly sampled crystals have the same pattern and similar interspot distance. Figure 3A is a representative of the TED patterns, exhibiting a 6-fold symmetric arrangement of sharp diffraction spots. Clearly, the hexagonal pattern indicates 6-fold projected symmetry in the colloidal crystals. Because the fcc, bcc, and hcp all exhibit the 6-fold projected symmetry, the the most direct way to distinguish a hexagonal-close-packing system from a cubic-close-packing system is to record the TED from at least two zone axes.[8,9] But this target can also be attained in this case by combining the XRD data, ED data, and deduction. By the combination of XRD data with TED data, the electron diffraction can only be indexed as the [0001] zone patterns of the hcp system with the parameter of $a = 5.25$ nm. The hexagonal structure system can fit the ED and XRD pattern completely and consistently. However, the TED pattern cannot be correctly indexed as the fcc structure with the parameter of $a = 7.46$ nm obtained from the XRD data. Although the TED pattern could be indexed as the cubic system with a parameter of $a = 12.98$ nm for fcc (or $a = 6.49$ nm for bcc), the XRD peaks could not be indexed using the same parameters. Therefore, the analysis and results suggest that the Au nanoparticles are uniquely stacked with a hexagonal close packing in the colloidal crystals. It can also be seen from the diffraction pattern that even the third-order diffraction spots are observable, suggesting the formation of perfect Au colloidal crystal on a large scale. HRTEM observation is also carried out to confirm the stacking behavior of Au nanoparticles in the colloidal crystals. Figure 3B presents the HRTEM image of a colloidal crystal and the superlattice fringes on the edge of the crystal are clear. The fringe spacing is measured to be ≈4.5 nm and this value is close to the d spacing of the lattice planes with the type of $\{10\bar{1}0\}$ (4.55 nm) in the hcp system, in agreement with the primary diffraction of small-angle TED.

In the hexagonal-close-packing model of hard spheres the unit cell parameter a is equal to the distance

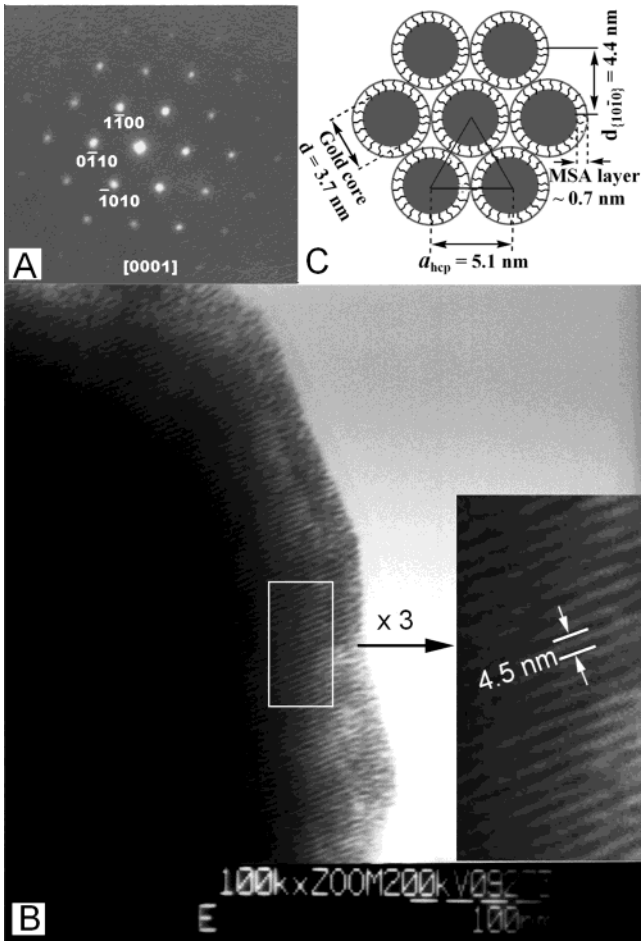

Figure 3. (A) Small-angle electron diffraction pattern recorded from an individual Au colloidal crystal with a camera length of 2.0 m and (B) high-resolution TEM image showing the supperlattice fringes of {10$\bar{1}$0} in the hcp system. The inset in (B) presents the enlargement of the boxed area. (C) shows the stacking model of Au nanoparticles viewed along the [0001] zone axis of the hcp system when the Au nanoparticles were treated as simple hard spheres.

between two adjacent spheres' centers. When the Au nanoparticles consisting of Au cores and MSA organic layer shells are treated as hard spheres, a stacking model can be drawn based on the above discussion and analysis. Figure 3C depicts the stacking behavior of the hexagonally packed Au nanoparticles viewed along the [0001] zone axis of the crystal. For simplicity, only a single layer of Au nanoparticles on the (000l) lattice plane is shown. The unit cell parameter a (≈5.1 nm) deduced from this stacking model is close to those (≈5.25 nm) obtained from XRD and TED experiment. The d spacing of {10$\bar{1}$0} (d = 4.4 nm) is also consistent with the HRTEM measurement (d = 4.5 nm).

Considering the carboxyl group tail of the coating MSA molecules in colloidal crystals, it can be assessed that the adjacent Au nanoparticles are interconnected by hydrogen bonding, either direct coupling among carboxyl groups or through water molecules. In the latter case, the distances among adjacent Au nanoparticles are apparently expanded. The coupling interactions among building Au nanoparticle units in the colloidal crystals are interesting because they can affect not only the stacking behavior of particles, consequentially affecting the final crystal structure, but also the electronic properties of the colloidal crystals. This study is in progress and will be reported in forthcoming publications.

In conclusion, well-developed, faceted, large Au colloidal crystals are prepared through a simple method in bulk aqueous media using the water-soluble Au nanoparticles as the starting material. The chemical composition of the Au colloidal crystals estimated by EDX contains mainly gold, carbon, oxygen, and sulfur elements, which is consistent with that of the starting materials. The crystallographic parameters are uniquely determined to be hexagonal close packing using TED and XRD techniques.

Acknowledgment. Financial support and granting of the postdoctoral fellowship (P01261) of this work from the Japan Society for Promotion of Science is gratefully acknowledged. The authors are indebted for support in part by Grants-in-Aid for Scientific Research (B: 13440212) from the Ministry of Education, Culture, Sports, Science and Technology. This study was also supported in part by the Hosokawa Powder Technology Foundation, the Mitsubishi Research Institute, and the Japan Space Utilization Promotion Center.

CM0217147